ARTICLES

Coarsening dynamics of a one-dimensional driven Cahn-Hilliard system

C. L. Emmott and A. J. Bray
Department of Physics and Astronomy, University of Manchester, Manchester, M13 9PL, United Kingdom
(Received 4 April 1996)

We study the one-dimensional Cahn-Hilliard equation with an additional driving term representing, say, the effect of gravity. We find that the driving field E has an asymmetric effect on the solution for a single stationary domain wall (or ''kink''), the direction of the field determining whether the analytic solutions found by Leung [J. Stat. Phys. **61**, 345 (1990)] are unique. The dynamics of a kink-antikink pair (''bubble'') is then studied. The behavior of a bubble is dependent on the relative sizes of a characteristic length scale E^{-1}, where E is the driving field, and the separation L of the interfaces. For $EL \gg 1$ the velocities of the interfaces are negligible, while in the opposite limit a traveling-wave solution is found with a velocity $v \propto E/L$. For this latter case ($EL \ll 1$) a set of reduced equations, describing the evolution of the domain lengths, is obtained for a system with a large number of interfaces and implies a characteristic length scale growing as $(Et)^{1/2}$. Numerical results for the domain-size distribution and structure factor confirm this behavior, and show that the system exhibits dynamical scaling from very early times. [S1063-651X(96)00511-9]

PACS number(s): 64.60.Cn, 75.40.Gb

I. INTRODUCTION

When a system is quenched from a homogeneous high-temperature phase into a two-phase region, domains of the new equilibrium phases form and evolve with time. The dynamics of systems described by a conserved order parameter, such as binary alloys or binary liquids undergoing phase separation, is conventionally modeled by the Cahn-Hilliard equation [1]. At late times after the quench, the domain coarsening is well described by a scaling phenomenology, with a single characteristic length scale $L(t)$.

Recently there has been much interest in the dynamics of phase separation in the presence of an external driving field [2–4], as this has applications to, for example, spinodal decomposition in a gravitational field. In order to capture the dynamics of a system in the presence of an external driving field, an order-parameter-dependent diffusion coefficient (or ''mobility'') is required [2,5,6]. The resulting modification of the Cahn-Hilliard equation has been studied by several authors both analytically and numerically [2,5–9]. In all the two-dimensional simulations the two phases form structures that align along the direction of the field, with different time dependences for the typical length scales parallel and perpendicular to the field. Analytic work on interfacial dynamics has revealed an instability in surfaces perpendicular to the field [2,10] that explain this configuration. However, given the complexity of the problem, no satisfactory scaling results have been obtained.

In order to obtain some qualitative understanding, we study in this paper the Cahn-Hilliard equation in one dimension. This system has been studied in the absence of a field by several authors [11–13]. In the presence of a field, analytic solutions have been obtained for a single interface in an infinite system [8]. In Sec. II we show, however, that these solutions are not unique. The direction of the field relative to the kink profile determines whether the analytical solution obtained by Leung [8] is unique or just one of a family of solutions. The work in Sec. II motivates the introduction of an additional characteristic length scale inversely proportional to the field strength [7].

In Sec. III the profile of kink-antikink pairs is studied numerically. The behavior of these systems is dependent on the relative values of the characteristic length E^{-1} and L, the distance between the interfaces. These systems are considered in two separate limits $EL \ll 1$ and $EL \gg 1$. For $EL \ll 1$, the kink-antikink pair form a traveling wave, moving at a speed proportional to E/L. For $EL \gg 1$, the domain walls are essentially frozen.

The limit $EL \ll 1$ is reconsidered in Sec. IV, in the context of a system with many interfaces. We consider the case in which all the domain lengths L_i satisfy $EL_i \ll 1$ and show that a simple effective dynamics for the interfaces can be constructed, in which the velocity of a given interface is proportional to the difference of the inverse lengths of the domains on either side of it. This then leads to a simple equation for the time evolution of the domain lengths themselves, from which it follows immediately that any characteristic length scale must grow as $\sqrt{t}$. Numerical simulations of the effective dynamics demonstrate scaling, with an average domain size growing as $\sqrt{t}$ as expected.

Section V concludes with a discussion and summary of the results.

II. SINGLE-INTERFACE SOLUTIONS OF THE CAHN-HILLIARD EQUATION

The phase-separation dynamics of a conserved system are modeled by the Cahn-Hilliard equation [1]

$$\frac{\partial \phi}{\partial t} = \nabla \cdot \left(\lambda \nabla \frac{\delta F}{\delta \phi} \right), \tag{1}$$

where $F[\phi]$ is the usual ϕ^4 Hamiltonian, but with an additional term to include the effects of the external field

$$F[\phi]=\int d^dx\left(\frac{1}{2}(\nabla\phi)^2+\frac{1}{4}(1-\phi^2)^2-\tilde{\mathbf{E}}\cdot\mathbf{x}\phi\right). \quad (2)$$

Throughout this paper only the deterministic Cahn-Hilliard equation is considered, i.e., the Langevin noise term has been omitted. This restricts the limits of validity of these results to temperature $T=0$ or, more generally, to T small enough that the effects of thermal fluctuations may be neglected.

If the mobility λ is independent of the order parameter, inserting (2) into (1) shows immediately that the term involving $\tilde{E}$ drops out of the dynamics. For nontrivial (and physical) results, therefore, the inclusion of an external field requires that the dependence of the mobility λ on the order-parameter field ϕ should be explicitly taken into account [2,5,6]. In this paper we take the simplest form for λ that maintains the symmetry under $\phi\rightarrow-\phi$, i.e., $\lambda=1-a\phi^2$. Hence rewriting Eq. (1) in one dimension and defining $a\tilde{E}=E$, we obtain

$$\frac{\partial\phi}{\partial t}=\frac{\partial^2\mu}{\partial x^2}+E\frac{\partial(\phi^2)}{\partial x}=-\frac{\partial J}{\partial x}, \quad (3)$$

where

$$\mu=\phi(\phi^2-1)-\phi''$$

is the chemical potential and J is the current. Note that we have only kept the leading-order term in a, as is conventional. Technically, this is equivalent to taking the limits $a\rightarrow0$ and $\tilde{E}\rightarrow\infty$, holding $E=a\tilde{E}$ fixed.

For an infinite system, analytic solutions to Eq. (3) have been found for a single stationary interface [8]. The order-parameter profile for a kink solution is given by

$$\phi(x)=\phi_\infty\tanh(\phi_\infty x/\sqrt{2}), \quad (4)$$

with

$$\phi_\infty^2=1+\sqrt{2}E, \quad (5)$$

valid for both signs of E. The corresponding antikink solution is obtained by inserting an overall minus sign in (4) and replacing E by $-E$ in (5). [This reflects the symmetry of (3) under $\phi\rightarrow-\phi$, $E\rightarrow-E$.]

In general, solutions to nonlinear equations are not unique. The aim of this section is to investigate the solutions of Eq. (3) numerically, and to present some simple analysis that accounts for the (at first sight surprising) results.

The continuum equation (3) was discretized on the interval $(-L/2,L/2)$ and antiperiodic boundary conditions $\phi(-L/2)=-\phi(L/2)$ were imposed. A kink solution was sought by using an antisymmetric tanh profile, with $\phi(0)=0$ and $\phi(L/2)>0$, as the initial condition. A range of initial values of $\phi(L/2)$ was used. This initial state was then evolved under the dynamics (3) until the system reached a stationary profile. A system size $L=500$ was used with a mesh size of 0.5. This value of L was found to be large enough that the results showed no finite-size effects. The time step used in the iteration was $\Delta t=0.005$.

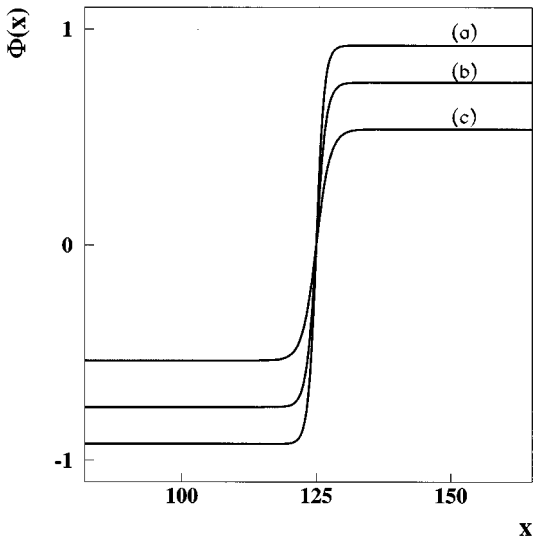

FIG. 1. Stationary single-interface solutions of Eq. (3). There is a unique solution for each $E<0$. (a) $E=-0.1$, (b) $E=-0.3$, and (c) $E=-0.5$.

It was found that the number and form of the stationary profiles found were strongly dependent on the sign of the field. For each negative field value a unique stationary wall profile was found, independent of the initial conditions used, i.e., of the initial value of $\phi(L/2)$. The final value of $\phi(L/2)$ obtained was found to be below the analytically predicted value $(1+\sqrt{2}E)^{1/2}$ [Eq. (5)]; the discrepancy vanished, however, as the mesh size was decreased (see Fig. 1).

For a positive field a family of solutions was found, with the final value of $\phi(L/2)$ equal to the initial value. The interface was found in general to be broader than for $E<0$, the asymptotic exponential decay to the value $\phi(L/2)$ occurring at a rate determined by the magnitude of the field, the decay rate decreasing as the field decreases. For larger values of the field, this exponential tail became oscillatory (see Fig. 2).

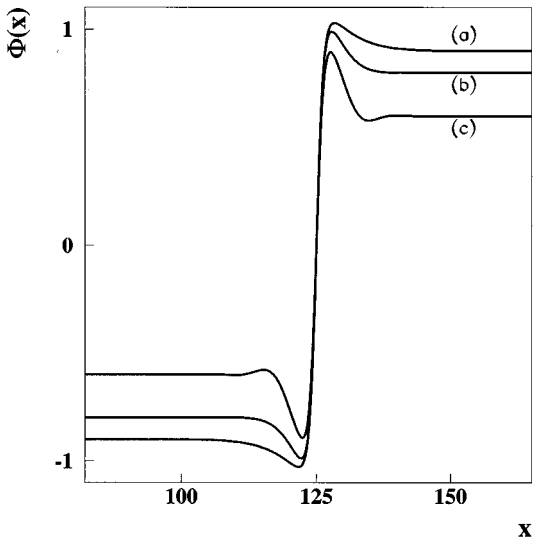

FIG. 2. Stationary single-interface solutions of Eq. (3). (a) $E=0.2$, (b) and (c) $E=0.3$: two examples from a family of solutions. For each value of the field there is a different decay length.

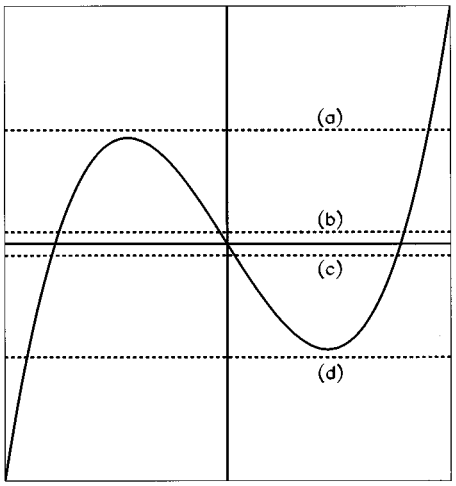

FIG. 3. Graphic solution (schematic) of Eq. (8) for the four cases discussed in the text.

Some simple analysis of the differential equation (3) can be used to explain some of these features. The existence of a solution representing a single interface in an infinite system is dependent on the choice of boundary conditions. For a physical solution, two of the boundary conditions imposed must be $\phi(0)=0$, which fixes the position of the interface, and $\phi''(0)=0$, a consequence of the antiperiodicity. The other two boundary conditions $\phi'(0)$ and $\phi(\infty)$ must be chosen to ensure the existence of a solution. This places constraints on the possible values of these variables. By the use of some simple stability analysis it is possible to deduce the type of constraints this places on $\phi'(0)$ and $\phi(\infty)$ and hence the number of values for which a solution exists.

Equation (3) can be integrated once to give a third-order differential equation

$$E\phi^2+(3\phi^2-1)\phi'-\phi'''=E\phi_\infty^2, \tag{6}$$

the integration constant $E\phi_\infty^2\equiv E\phi^2(\pm\infty)$ ensuring that $\phi(x)$ tends to a constant value at infinity. Linearizing around this value for large positive x, $\phi(x)=\phi_\infty+\tilde{\phi}(x)$, gives

$$\tilde{\phi}'''+(1-3\phi_\infty^2)\tilde{\phi}'-2E\phi_\infty\tilde{\phi}=0. \tag{7}$$

It follows that $\tilde{\phi}$ will have solutions of the form $\exp(\lambda x)$, where the possible values of λ are the roots of the cubic equation

$$\lambda^3+(1-3\phi_\infty^2)\lambda=2E\phi_\infty. \tag{8}$$

The nature of the roots of this equation is dependent on the values of ϕ_∞ and E.

Note that in the present discussion we are taking $\phi(\infty)>0$ and considering both signs of E. This means that we are dealing with a kink, not an antikink. Later, when we consider systems with both kinks and antikinks, we will fix $E>0$. Since, however, the equation of motion (3) is invariant under $E\to-E$, $\phi\to-\phi$, it follows that the properties of an antikink for $E>0$ are identical to those of a kink for $E<0$. In the following stability analysis, therefore, we restrict the discussion to kinks.

There are four cases to consider, as illustrated in Fig. 3.

(a) $E>0$ and $(E\phi_\infty)^2>(\phi_\infty^2-\frac{1}{3})^3$. Two roots are complex with negative real parts and the third root is real and positive.

(b) $E>0$ and $(E\phi_\infty)^2<(\phi_\infty^2-\frac{1}{3})^3$. All roots are real: one positive and two negative. For $E\to0$, $\phi_\infty\to1$ and the roots are $\lambda\approx\pm\sqrt{2},-E$.

(c) $E<0$ and $(E\phi_\infty)^2<(\phi_\infty^2-\frac{1}{3})^3$. All roots are real: one negative and two positive. For $E\to0$, the roots are $\lambda\approx\pm\sqrt{2},-E$.

(d) $E<0$ and $(E\phi_\infty)^2>(\phi_\infty^2-\frac{1}{3})^3$. Two roots are complex with positive real parts and the third root is real and negative.

For $x\to\infty$, the function $\tilde{\phi}(x)$ has the form

$$\tilde{\phi}(x)=\sum_{i=1}^{3}a_i\exp(\lambda_i x).$$

The coefficients a_i are fixed by the initial conditions and the value of ϕ_∞. Linear stability of the putative solution with $\phi(x)\to\phi_\infty$ as $x\to\infty$ requires that $\tilde{\phi}$ vanish at infinity, i.e., the coefficients a_i corresponding to eigenvalues λ_i with positive real part must vanish.

To see what this implies, consider integrating the third-order equation (6) with the initial conditions $\phi(0)=0=\phi''(0)$, which follow from the antisymmetry of the solution, and some fixed $\phi'(0)$. One also needs to specify the value of the parameter ϕ_∞ appearing in the equation. The two parameters $\phi'(0)$ and ϕ_∞ must be varied until the solution $\phi(x)$ approaches the same value ϕ_∞ as $x\to\infty$. If the input values deviate slightly from the correct values, the solution will ultimately diverge from ϕ_∞ due to the presence of unstable modes (with $\mathrm{Re}\lambda_i>0$) in the linearized solution for $\tilde{\phi}$. To ensure that such diverging terms are absent, the parameters $\phi'(0)$ and ϕ_∞ have to be adjusted until the corresponding coefficients a_i vanish. This is the familiar ''shooting method'' of solving nonlinear differential equations.

For $E>0$ there is only one unstable mode. Hence, for solutions to exist only one coefficient must vanish, imposing a constraint of the form $a_1[\phi'(0),\phi_\infty]=0$. This defines a line in parameter space for which this coefficient vanishes, resulting in a range of possible values for ϕ_∞. One therefore expects a family of solutions, parametrized by ϕ_∞, for $E>0$.

For $E<0$, however, there are two roots with positive real parts. Therefore the coefficients of both unstable modes are required to vanish. Hence the only choice for the parameters ϕ_∞ and $\phi'(0)$ for which a solution exists is at the intersection of the two lines defined by setting both coefficients to zero, i.e., $a_1[\phi'(0),\phi_\infty]=0=a_2[\phi'(0),\phi_\infty]$. This results in a unique solution for $E<0$.

The values of E and ϕ_∞ determine whether the roots of the cubic equation (8) are real or complex. The existence of complex roots with negative real parts for E sufficiently large and positive [case (a) in Fig. 3] results in oscillatory behavior.

For a given stable solution, the eigenvalue λ with the least-negative real part determines the rate of the asymptotic exponential decay towards ϕ_∞. For E small and positive,

this eigenvalue is $-E$. Hence, for $E>0$, the value of E determines a characteristic length in the system E^{-1}, which defines the width of any boundary effect at an interface. This characteristic length is important when considering systems with more than one interface as in the following sections. For $E<0$, by contrast, there is only one negative eigenvalue, which approaches a nonzero limiting value for $E\to 0$: the width of a kink for $E<0$ therefore remains of order unity for small E.

How do we interpret the analytic kink solution (4) in the light of the foregoing discussion? For $E<0$, the analytic solution is the unique solution we predict. For $E>0$, we have argued for (and numerically demonstrated) a family of solutions. Which one corresponds to Eq. (4)? It is easy to show that the exponential decay of (4) to ϕ_∞ as $x\to\infty$ is governed by the more negative of the two negative eigenvalues arising from the stability analysis. The exact solution (4) therefore corresponds to the case where the amplitude a corresponding to the least negative eigenvalue vanishes, i.e., to just one member of the family of solutions.

Throughout this section we have considered only kink solutions ($\phi>0$ at positive infinity) and allowed E to take either sign. We conclude by interpreting our results for the physically relevant case where the sign of E is fixed (we take $E>0$) and both kinks and antikinks are present. From the symmetry of the dynamics under $\phi\to-\phi$, $E\to-E$, it follows that for $E>0$ there is a family of kink solutions, but a unique antikink solution. In a system with well-separated (relative to E^{-1}) kinks and antikinks, however, continuity of the function ϕ will select the kink solution that matches smoothly the unique antikink solution. When the kink-antikink separation is small compared to E^{-1}, more interesting behavior is possible. This is the subject of the next section.

III. SINGLE-BUBBLE SOLUTIONS OF THE CAHN-HILLIARD EQUATION

In this section solutions to the Cahn-Hilliard equation for a kink-antikink pair in a periodic system are considered. The kink-antikink pair is a bubble of plus phase moving in a sea of minus phase. The velocities of the interfaces were investigated for various field strengths and kink-antikink separations.

The work in the preceding section produced a characteristic length E^{-1}, which determines (for a kink) the width of any boundary effect present at an interface. In the systems considered in this section there is a second important characteristic length L, the distance between the two interfaces. The behavior of these systems is dependent on the relative values of these two characteristic lengths. In this section we will consider two limits: first the case where $EL\gg 1$ and then the opposite limit $EL\ll 1$. The results from the second regime motivate a simple model for the many-interface problem, which is dealt with in Sec. IV.

A. $EL\gg 1$

The numerical solutions found for a kink-antikink pair in this limit are stationary. The value of the order parameter between interfaces was dependent only on the value of the field and was numerically found to be consistent with $\phi\approx\pm(1-\sqrt{2}E)^{1/2}$, the value given for an antikink by the analytical solution (4). Some examples of the profiles found are shown in Fig. 4.

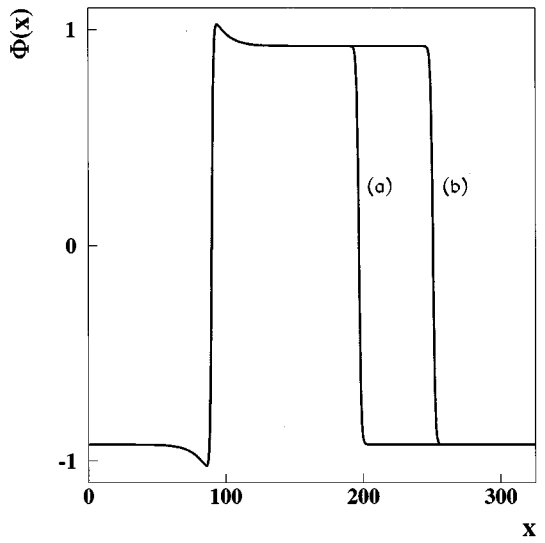

FIG. 4. Kink-antikink solutions with $L\approx 107$ and $L\approx 161$, for $E=0.1$, corresponding to the limit $EL\gg 1$.

These results can be explained using the results of Sec. II. If we assume that the system will reach a steady state and the order parameter may be written as a traveling wave $\phi=\phi(x-vt)$, then the Cahn-Hilliard equation (3) may be integrated once to obtain

$$E\phi^2+(3\phi^2-1)\phi'-\phi'''=J_0-v\phi, \tag{9}$$

where J_0 is a constant of integration and v is the wave velocity. In the limit $EL\gg 1$ the order parameter is approximately constant both inside and outside the bubble $\phi\approx\pm(1-\sqrt{2}E)^{1/2}$. Inserting this into the above equation in these regions and demanding that it hold inside domains of both sign, it is clear that one must have $J_0=E(1-\sqrt{2}E)$ and $v=0$. Therefore the solution is stationary, and since in this limit the separation L of the interfaces is large compared to E^{-1}, the profile is the combination of two single-interface solutions.

For one of the interfaces there exists a family of solutions for a fixed value of the field, whereas the other interface has a unique solution with a plateau height given by $\pm(1-\sqrt{2}E)^{1/2}$. This specifies the boundary conditions for the first interface, hence picking out one from the family of solutions.

B. $EL\ll 1$

In this limit the system was found numerically to evolve to a steady state with a fixed profile moving at a finite velocity. This may be shown by a comparison of the order parameter with the current, since for a traveling-wave solution Eq. (3) gives $-v\phi'=-J'$. Therefore the order parameter will be a multiple of the current J plus an overall constant. This expectation is confirmed by the data presented in Fig. 5.

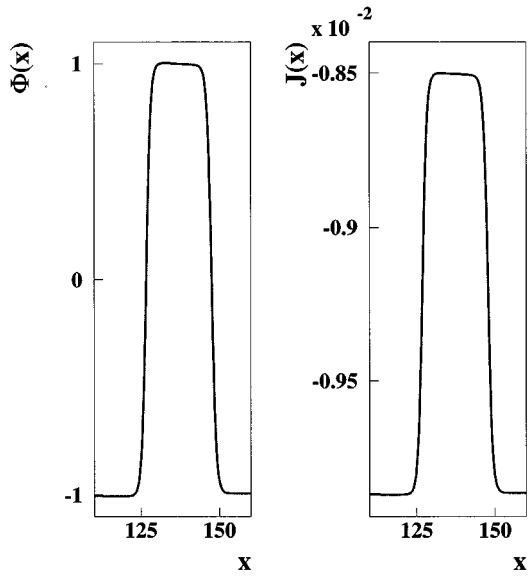

FIG. 5. Comparison between the order-parameter profile and the current for a kink-antikink pair of size $L \approx 21$, for $E = 0.01$, corresponding to the limit $EL \ll 1$.

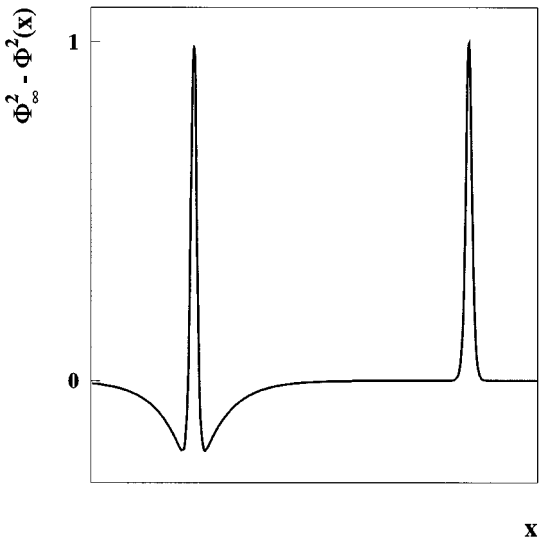

FIG. 6. Plot (schematic) of $\phi_\infty^2 - \phi^2(x)$ for a kink-antikink pair in the limit $EL \gg 1$. The total area under the curve is zero.

As in the previous limit, a long-range boundary effect exists at the kink interface, with the order parameter decaying exponentially to a fixed value outside the bubble. However, since $EL \ll 1$ the full exponential tail on the other side of the interface (i.e., between the two interfaces) is missing and the order parameter varies roughly linearly between the two interfaces, through a height difference proportional to the field. This linear regime between the interfaces is evident in Fig. 5.

Using the assumption (verified numerically) that the solution may be written as a traveling wave, Eq. (9) becomes

$$E(\phi^2 - \phi_\infty^2) + (3\phi^2 - 1)\phi' - \phi''' + v(\phi + \phi_\infty) = 0, \quad (10)$$

where $-\phi_\infty$ is the value of the order parameter in the minus phase far from the interfaces. The integration constant J_0 in (9) was fixed in (10) by the requirement $\phi(\pm\infty) = -\phi_\infty$. Integrating this equation over the whole system yields an expression for the velocity

$$v = E\frac{\int dx(\phi_\infty^2 - \phi^2)}{\int dx(\phi_\infty + \phi)} = \frac{E}{2\phi_\infty L}\int dx(\phi_\infty^2 - \phi^2), \quad (11)$$

where the final result follows from noting that $\phi \simeq \phi_\infty$ inside the bubble and $-\phi_\infty$ outside.

The function $\phi_\infty^2 - \phi^2$ is peaked at the interfaces. This can be used to explain why a finite velocity is expected. Consider first the case $EL \gg 1$, for which we showed above that the velocity is zero. For this case, therefore, $\int dx(\phi_\infty^2 - \phi^2)$ must be zero. Since the kink and antikink are well separated and the order parameter saturates at the value ϕ_∞ in the intermediate plateau region, $\int dx(\phi_\infty^2 - \phi^2)$ is a sum of kink and antikink contributions. One of the interfaces, corresponding to the antikink, is known analytically [from Eq. (4)] and the contribution it makes to the integral is $2\sqrt{2}\phi_\infty$. The contribution from the kink interface therefore must give an overall negative contribution of $-2\sqrt{2}\phi_\infty$. This is possible because, as is clear from Fig. 4, the kink solution overshoots ϕ_∞ and approaches the plateau at ϕ_∞ from the ''wrong'' side. The function $\phi_\infty^2 - \phi^2$ for the kink therefore contains both positive and negative regions, as shown in Fig. 6. The negative regions evidently contain the larger area [note that, although the magnitude of $\phi_\infty^2 - \phi^2$ in these regions is $O(E)$, the decay constant is also $O(E)$, leading to an area of $O(1)$] in such a way that the integral for the kink interface is precisely $-2\sqrt{2}\phi_\infty$.

Consider now the case $EL \ll 1$. In this case, the interior of the bubble is too small to contain the full exponential tail from the kink. The contributions from the kink to $\int(\phi_\infty^2 - \phi^2)$ will therefore be less negative than when $EL \gg 1$, resulting in a net positive value for the integral and, via (11), a positive bubble velocity, $v \propto E/L$. Therefore, in this limit the interfaces evolve to a fixed profile that moves with a velocity $v \propto E/L$. The qualitative tendency of smaller bubbles to move faster than larger ones was noted by Yeung *et al.*, on the basis of numerical studies [2].

We can make this argument quantitative in the limit of small E, for which $\phi_\infty \to 1$. In this limit, the area under the kink peak in Fig. 6 approaches the same value $2\sqrt{2}$ as the area under the antikink. The negative region between the two peaks is completely suppressed, as the decay length $1/E$ is much larger than the separation L of the peaks. The negative contribution from the semi-infinite region to the left of the kink peak, however, retains the value $-2\sqrt{2}$. The total area under the kink is therefore zero and the area under the kink-antikink pair is $2\sqrt{2}$. Equation (11) then gives a velocity $v = \sqrt{2}E/L$ for $E \to 0$. Applying this result to the data of Fig. 5, for which $E = 0.01$ and $L = 20.88$ (measured between the zeros of ϕ), gives $v = 6.77 \times 10^{-4}$, which compares well with the measured velocity of 6.82×10^{-4}.

The results of this section will be used in Sec. IV to derive the set of reduced equations employed to simulate a multidomain system. As a first step in generalizing this approach to many domains, we express the single-bubble cal-

culation in the limit $EL \ll 1$ in terms of currents. From Eq. (3), the current J can be written, up to an overall constant, as

$$J = -\mu' - E\phi^2 = \phi''' + (1-3\phi^2)\phi' - E\phi^2. \qquad (12)$$

The velocity of an interface is related to the discontinuity in the current at the interface [1] $v = \Delta J/\Delta\phi$, where ΔJ and $\Delta\phi$ are the discontinuities in the current and the order parameter, respectively. For a bubble that moves without change of shape (a traveling wave), J must have different values $J_{\rm in}$ and $J_{\rm out}$ inside and outside the bubble. To lowest order in E, we can write $\phi^2 = \phi_\infty^2 = 1$ both inside and outside, so that (12) becomes $J = \phi''' - 2\phi' - E$ in both regions. Outside the bubble, far from the interfaces, ϕ is constant, so $J_{\rm out} = -E$. Inside, the order parameter changes by an amount of order E over a distance L, so we estimate $\phi' = -E/L$ (and ϕ''' is negligible), giving $J_{\rm in} \sim -E + O(E/L)$ correct to $O(E)$. Finally, both interfaces have the same velocity $v \sim E/L$, in agreement with our earlier result (11) based on the traveling-wave solution. This second approach is, however, readily generalizable to the multidomain situation in the small-E limit.

IV. MANY-INTERFACE MODEL

In this section a set of reduced equations is derived using the work of the preceding section to describe the dynamics of a large number of interfaces in a periodic system. This reduced dynamics is numerically simulated, and the average domain length, domain-size distribution function, and structure factor are calculated.

We consider the case in which $EL_i \ll 1$ for all domains i, where the L_i are the domain lengths. From the arguments of the preceding section, we expect that, in this limit, $\phi' \sim -E/L_i$ in domain i and that the current J_i in domain i is given, up to an additive constant, by $J_i \propto E/L_i$. The proportionality constant in this relation is the same for all domains (an extension of the argument given above for the kink-antikink pair [15] gives its value as $4\sqrt{2}$).

Let us define interface i to have domain length L_i to its right and L_{i-1} to its left. If the interface is a kink ($\Delta\phi > 0$) its velocity v_i is

$$v_i^k = \frac{\Delta J}{\Delta\phi} \propto E\left(\frac{1}{L_i} - \frac{1}{L_{i-1}}\right). \qquad (13)$$

For an antikink ($\Delta\phi < 0$) the velocity v_i^{ak} is given by the same expression, but with a factor -1. If we arbitrarily assign even i to domains of positive ϕ, the equation for the time evolution of the domain length $dL_i/dt = (v_{i+1} - v_i)$ becomes

$$\frac{dL_i}{dt} = (-1)^i E\left(\frac{1}{L_{i-1}} - \frac{1}{L_{i+1}}\right), \qquad (14)$$

where an overall constant has been absorbed into the time scale. It follows immediately that, if L is a typical domain length, $dL/dt \sim E/L$, i.e., $L(t) \sim (Et)^{1/2}$.

The dynamics of the system was studied numerically using this set of reduced equations. The system was initially prepared with 100 000 domains with approximately equal amounts of the plus and minus phases. The field E was absorbed into the time scale, i.e., we set $E = 1$ in (14). The time step used in the iteration was $\Delta t \propto t$. This was chosen because we expect $t^{1/2}$ (i.e., power-law) growth. Then the $\Delta t \propto t$ leads to $\Delta L \propto L$, i.e., domains typically change length by a fixed (small) fraction of the mean length in each update. Similarly, domains were annihilated if the distance between interfaces became smaller than a specified (small) fraction of the average domain size. In the calculation of the average domain size and the domain-size distribution function, results were averaged over ten runs. It was found that the average domain size $\langle L(t)\rangle$ grew as $\sqrt{t}$, as expected (Fig. 7). The simulation results show that the distribution function $P(L,t)$ (the fraction of domains which have size L at time t) scales well from quite early times (Fig. 8). The scaling function was

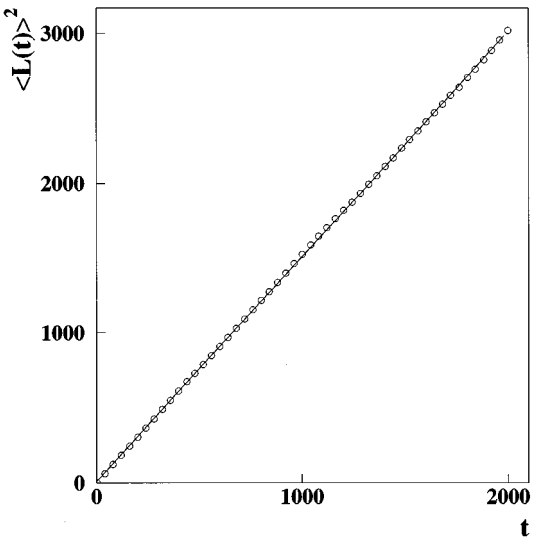

FIG. 7. Time dependence of the square of the average domain length for the dynamics described by Eq. (14). The mean domain size grows as $t^{1/2}$.

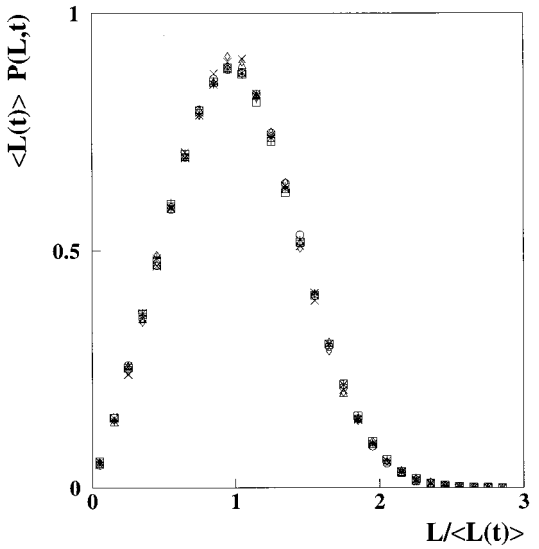

FIG. 8. Scaled domain-size distribution function for the dynamics described by Eq. (14). The data correspond to times 10 (□), 20 (+), 40 (*), 80 (○), 160 (×), 320 (△), and 640 (◇).

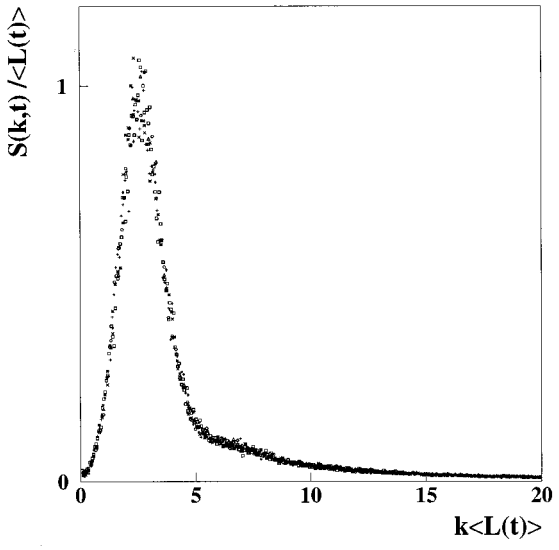

FIG. 9. Scaled structure factor for the dynamics described by Eq. (14). The data correspond to times between 10 and 640, as in Fig. 8.

found to be linear at the origin, with a Gaussian tail. However, we were unable to calculate it analytically.

Figure 9 shows the structure factor. This was taken as an average of 500 runs. The scaling collapse is good except near the peak, where the data are noisy. A ln-ln plot (Fig. 10) shows that in the limit $k\langle L\rangle \gg 1$ the structure factor possesses the expected Porod tail $S(k,t)\propto k^{-2}$. The constant of proportionality is determined by the average domain-wall density [1] $S(k,t)=4\rho k^{-2}$. Hence we would expect a ''Porod plot'' of $k^2\langle L\rangle S(k,t)$ to tend to the value 4 at large $k\langle L\rangle$. The data, although noisy in this regime, are consistent with this expectation.

The small-k data in Fig. 10 suggest the quadratic dependence $S(k,t)\propto k^2$. We can show that this is the correct small-

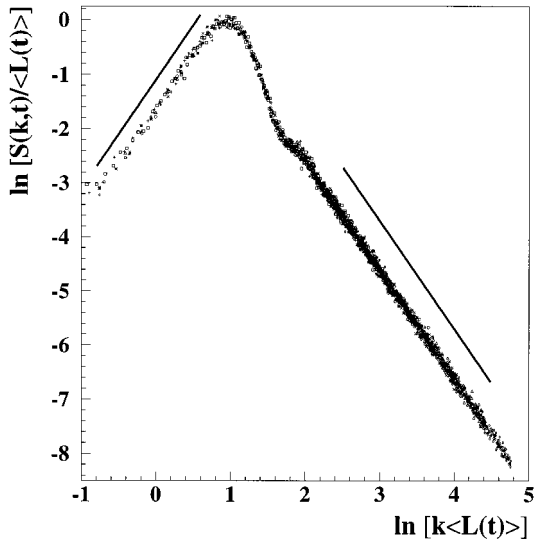

FIG. 10. Double-logarithmic plot of the scaled structure factor. Times between 10 and 640 are shown, as in Fig. 8. The straight lines in the small-$k\langle L\rangle$ and large-$k\langle L\rangle$ regimes have gradients 2 and -2, respectively. The latter is the expected Porod regime; an argument for the former is given in the text.

k behavior, following the methods used to establish the k^4 small-k behavior [1,14] for the nondriven Cahn-Hilliard equation in dimensions $d>1$.

For $k\to 0$, Eq. (3) can be written in Fourier space as

$$\frac{d\phi_k}{dt}=iEk(\phi^2)_k, \tag{15}$$

where the term of order k^2 is negligible and has been omitted. Integrating with respect to t, multiplying by ϕ_{-k}, and averaging gives the structure factor

$$S(k,t)=-S(k,0)+2\langle\phi_k(t)\phi_{-k}(0)\rangle + E^2k^2\int_0^t dt_1\int_0^t dt_2\langle(\phi^2[t_1])_k(\phi^2[t_2])_{-k}\rangle. \tag{16}$$

Since $S(k,t)$ has the scaling form $S(k,t)=Lg(kL)$, where L is shorthand for $\langle L\rangle$, it follows that $S(k,0)$ is negligible compared to $S(k,t)$ at late times (large L) and can be neglected. Similarly, $\langle\phi_k(t)\phi_{-k}(0)\rangle$ has the scaling form [1] $L^{\lambda}h(kL)$, where $\lambda<d/2=1/2$ follows from the Cauchy-Schwarz inequality [16], so this term can also be dropped for large L.

Next we consider the equal-time correlation function $D(r,t)=\langle[\phi_\infty^2-\phi^2(x)][\phi_\infty^2-\phi^2(x+r)]\rangle$. It's Fourier transform is the equal-time version of the quantity required in (16). The function $\rho(x)\equiv\phi_\infty^2-\phi^2(x)$ vanishes except near domain walls, so it is essentially a domain-wall density function, with δ-function contributions from the walls [15]. It follows that $\langle\rho\rangle\sim 1/L$, the mean domain-wall density, while $D(r,t)$ has the scaling form $D(r,t)=L^{-2}f_D(r/L)$. The two-time generalization is $D(r,t_1,t_2)=L_1^{-2}f_D(r/L_1,L_2/L_1)$, where $L_1\equiv L(t_1)$. The spatial Fourier transform required in (16) has the form $T(k,t_1,t_2)=L_1^{-1}g_D(kL_1,L_2/L_1)$, which reduces to $L_1^{-1}h(L_2/L_1)$ in the limit $k\to 0$ (we do not expect T to vanish in this limit, because ρ is not a conserved quantity).

If $L(t)$ grows as a power of t, the double time integral in (16) gives, up to constants, t^2/L, so the right-hand side of (16) is of order $E^2k^2t^2/L$. Requiring that $S(k,t)=Lg(kL)$ have the same small-k form gives $S(k,t)\sim k^2L^3$ and hence $L\sim(Et)^{1/2}$. It is reassuring that this form for $L(t)$ agrees precisely with that obtained from the reduced dynamics (14).

V. CONCLUSION

We have studied, analytically and numerically, the effect of an external driving field on the coarsening dynamics of the one-dimensional Cahn-Hilliard equation at $T=0$. For a single stationary interface, it was shown that the direction of the field for a domain wall of a given sign determines whether there is a unique solution or a family of solutions. In the latter case, the approach of the interface profile function to its asymptotic value is governed by an exponential tail with a decay constant that vanishes linearly with the driving field E. There is therefore a new characteristic length scale E^{-1} in this system.

The behavior of a kink-antikink pair (''bubble'') falls into two classes, characterized by the relative values of the inter-

face separation L and the new characteristic length E^{-1}. In the limit $EL \gg 1$, the bubble profile is stationary. In the opposite limit $EL \ll 1$, a bubble of plus phase moves through the minus phase with a velocity $v \propto E/L$.

For the many-domain coarsening dynamics an equation of motion for the domain lengths was derived [Eq. (14)], valid in the regime $EL \ll 1$, in which the length of a given domain changes at a rate determined by the lengths of the domains on either side. The mean domain size grows as $\sqrt{Et}$. Despite the apparent simplicity of this model, we have so far been unable to make further analytical progress. Numerical simulations, however, demonstrate dynamic scaling (for the domain-size distribution and the structure factor) and confirm the predicted $\sqrt{t}$ growth law. An argument for the observed k^2 behavior of the structure factor at small k has been presented.

It would be interesting to compare the dynamics of this effective model to that of the original driven Cahn-Hilliard equation. There are practical obstacles, however, to a simulation of the full dynamics. To ensure that the condition $EL \ll 1$ is satisfied at all times, a small value of E is required, leading to very slow growth, whereas in the reduced model the value of E factors out. Furthermore, updating the field everywhere in space is computationally very inefficient, especially at late times, compared to just updating the domain lengths. Systems large enough to support the 10^5 initial domains used in the reduced dynamics (and needed for good statistics) would require prohibitively large computer time.

We have shown that the mean domain size L grows as $\sqrt{Et}$ when the condition $L \ll 1/E$ is satisfied. For E strictly zero, however, logarithmic growth of L with time is obtained [11], so the question of the crossover as $E \to 0$ arises. In our treatment, the typical interface velocity is of order E/L, whereas for $E=0$ it is of order μ/L, where the chemical potential μ is of order $\exp(-\text{const}L)$ [13]. The crossover between these two forms occurs when $L \sim \ln(1/E)$, so the validity of our approach strictly requires $\ln(1/E) \ll L \ll 1/E$. For small E, of course, this regime is very broad.

In a related work, the one-dimensional Ising model with Kawasaki spin-flip dynamics, biased in one direction, has been studied [17]. Numerical results were obtained for a range of volume fractions, including the case of equal volume fractions simulated here, and $\sqrt{t}$ growth demonstrated. There, as here, rather general arguments lead to $\sqrt{t}$ growth for all volume fractions: for the present model from the dimensional analysis of Eq. (14). For the Ising model, however, exact results for the domain-size distribution (and for the ''persistence exponent'' [17]) were obtained in the limit where one phase occupies a negligible volume fraction, so it is interesting to consider the present model in this same limit.

When one phase (the plus phase, say) occupies a very small volume fraction, the system consists of domains of plus phase separated by (typically) much larger domains of minus phase. To a first approximation, therefore, each plus domain can be treated as an isolated bubble in the sense of Sec. III. Each such bubble then moves at a speed E/L, where L is its length (we are taking $EL \ll 1$ here), all bubbles moving in the same direction. As a result, small bubbles catch up with larger bubbles, with which they then merge, and the combined domain slows down. Just before the bubbles merge, the approximation of treating them as independent breaks down when the size of the intervening minus domain becomes comparable with the size of the bubbles. This presumably leads to negligible corrections to the scaling functions, however, in the small volume-fraction limit. This new model is so simple that analytic progress may be possible. However, we will leave this question for future work.

ACKNOWLEDGMENTS

C.L.E. would like to thank Sarah Phillipson for useful discussions and EPSRC (United Kingdom) for support.

[1] For a recent review of phase-ordering kinetics, see A. J. Bray, Adv. Phys. **43**, 357 (1994).
[2] C. Yeung, T. Rogers, A. Hernández-Machado, and D. Jasnow, J. Stat. Phys. **66**, 1071 (1992).
[3] S. Puri, K. Binder, and S. Dattagupta, Phys. Rev. B **46**, 98 (1992); S. Puri, N. Parekh, and S. Dattagupta, J. Stat. Phys. **75**, 839 (1994).
[4] F. J. Alexander, C. A. Laberge, J. L. Lebowitz, and R. K. P. Zia, J. Stat. Phys. **82**, 1133 (1996).
[5] C. Yeung, J. L. Mozos, A. Hernández-Machado, and D. Jasnow, J. Stat. Phys. **70**, 1149 (1993).
[6] K. Kitahara, Y. Oono, and D. Jasnow, Mod. Phys. Lett. B **2**, 765 (1988).
[7] K. Leung, J. Stat. Phys. **50**, 405 (1988).
[8] K. Leung, J. Stat. Phys. **61**, 345 (1990).
[9] A. M. Lacasta, A. Hernández-Machado, and J. M. Sancho, Phys. Rev. B **48**, 9418 (1993).
[10] A. Hernández-Machado and D. Jasnow, Phys. Rev. A **37**, 656 (1988).
[11] T. Kawakatsu and T. Munakata, Prog. Theor. Phys. **74**, 11 (1985).
[12] K. Kawasaki and T. Ohta, Physica **116A**, 573 (1982).
[13] S. N. Majumdar and D. A. Huse, Phys. Rev. E **52**, 270 (1995).
[14] H. Furukawa, J. Phys. Soc. Jpn. **58**, 216 (1989); Phys. Rev. B **40**, 2341 (1989); Prog. Theor. Phys. Suppl. **99**, 358 (1989).
[15] For the many-interface situation considered here, the exponential tails of the kink profiles are cut off on both sides by the neighboring antikinks (for $EL \ll 1$), so the function $\phi_\infty^2 - \phi^2(x)$ has peaks with positive (and essentially the same) area for both kinks and antikinks.
[16] C. Yeung, M. Rao, and R. C. Desai, Phys. Rev. E **53**, 3073 (1996).
[17] S. J. Cornell and A. J. Bray, Phys. Rev. E **54**, 1153 (1996).